

BUCKLING OF RADIALLY CONSTRAINED CIRCULAR RING UNDER DISTRIBUTED LOADING†

T. H. H. PIAN and L. L. BUCCIARELLI, JR.

Department of Aeronautics and Astronautics, Massachusetts Institute of Technology,
Cambridge, Massachusetts

Abstract—The paper presents first an approximate solution of the static, elastic deformation of a thin circular ring which is constrained in a rigid circular boundary and is acted upon by uniformly distributed loading along a direction in the plane of the ring. The solution is based on the assumption that the detached region is limited to a small portion of the circumference. The result of the solution is represented by a load-deflection curve which indicates the snap-buckling behavior of the ring.

The system of nonlinear equation for the exact formulation has also been studied. A systematic iterative scheme is developed for its solution and is applied to a ring of R/t equal to 100. The result compares favourably with the approximate solution.

INTRODUCTION

IN this paper we consider an elastic thin ring (Fig. 1), constrained, but unbonded, inside a rigid circular boundary. The ring lies in a vertical plane and is acted upon by a vertical

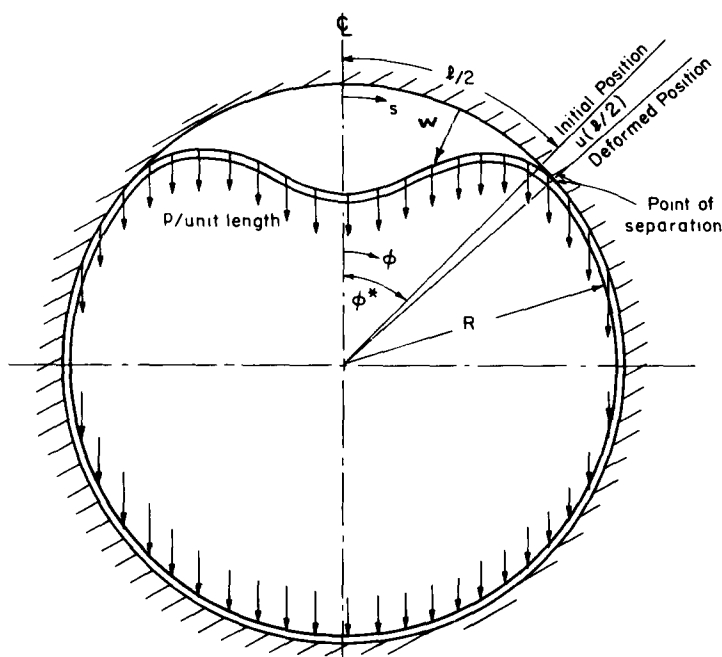


FIG. 1. Radially constrained circular ring under distributed vertical loading.

† The work described in this paper was sponsored by the Air Force Office of Scientific Research. The work was completed during the senior author's affiliation with the California Institute of Technology in his year of sabbatical leave from the Massachusetts Institute of Technology.

distributed loading. As a preliminary study here we maintain the conservative nature of the problem by assuming that there is no friction between the ring and the rigid wall. We also limit our investigation to the deformation mode which is symmetrical with respect to the vertical axis. Our objective is to determine the tangential and radial inward displacements of the ring at different loading amplitudes and to predict the condition under which snap-buckling will occur.

It is seen that under distributed downward loading the upper portion of the ring will separate from the wall while the bottom portion remains attached. The present problem is complicated by the fact that the location of the point of separation is an unknown. It is obvious that for the problem of snap-buckling a large deflection theory is required for the analysis of the detached region. As will be shown in the large deflection analyses contained in this paper, the extent of the detached region is a function of the loading magnitude.

The first part of this paper deals with an approximate solution of the problem. A second section is devoted to the exact solution of the limiting case of small deflections. Finally, the exact formulation of the large deflection problem and a brief description of its solution by numerical means are presented. A detailed account of the numerical solution may be found in [1].

APPROXIMATE SOLUTION †

To obtain an approximate solution of the present problem we limit our consideration to the case in which (i) the detached portion of the ring subtends an angle of less than 50° ; (ii) strains are small but displacements and rotations are only moderately small. For this particular situation, the one dimensional equivalent of the Marguerre nonlinear shallow shell equations provide a suitable analytical description of ring behavior. The equilibrium equations with respect to the deformed configuration reduce to:

$$\frac{dN}{ds} = 0; \quad \text{or } N = \text{constant}$$

$$\frac{d^2M}{ds^2} + N \left(\frac{1}{R} + \frac{d^2w}{ds^2} \right) - p = 0 \tag{1}$$

where

N = circumferential force, positive in compression

M = bending moment

R = radius of the ring

s = coordinate along the circumference with its origin at the top of the ring

w = radial displacement of the ring, positive inward

p = distributed load per unit length.

† After the submission of this manuscript the authors have learned that E. A. Zagustin and G. Herrmann have also obtained an approximate solution of this problem, with results identical to the present investigation. Their paper entitled "Stability of an Elastic Ring in a Rigid Cavity" will be published in the *Journal of Applied Mechanics*.

The bending moment is related to the curvature by

$$\frac{d^2w}{ds^2} = \frac{M}{EI} \quad (2)$$

where EI is the bending rigidity of the ring, we obtain the following differential equation for M :

$$\frac{d^2M}{ds^2} + \frac{N}{EI}M = -\frac{N}{R} + p. \quad (3)$$

The solution is

$$M = C_1 \sin ks + C_2 \cos ks - EI(1 - \beta)/R \quad (4)$$

where

$$k = \sqrt{(N/EI)} \quad (5)$$

$$\beta = pR/N. \quad (6)$$

Now the attached portion of the ring behaves effectively as a membrane. The bending moment then vanishes there. Hence $M(\pm l/2) = 0$. Under these conditions, equation (4) becomes

$$M = \frac{EI(1 - \beta)}{R} \left[\frac{\cos ks}{\cos(kl/2)} - 1 \right]. \quad (7)$$

Substituting into equation (2) and integrating, we obtain

$$\frac{dw}{ds} = \frac{(1 - \beta)}{R} \left[\frac{\sin ks}{k \cos(kl/2)} - s \right] + C_1 \quad (8)$$

and

$$w = \frac{(1 - \beta)}{R} \left[-\frac{\cos ks}{k^2 \cos(kl/2)} - \frac{s^2}{2} \right] + C_1 s + C_2. \quad (9)$$

The boundary conditions of $w(\pm l/2) = 0$ yield

$$w = \frac{(1 - \beta)}{R} \left[\frac{1}{k^2} \left(1 - \frac{\cos ks}{\cos(kl/2)} \right) - \frac{s^2}{2} + \frac{l^2}{8} \right]. \quad (10)$$

It is seen that the solution is symmetric about the mid-point of the detached region.

We note further that the derivative dw/ds should also vanish at $s = \pm l/2$. By applying either condition we obtain the following relation:

$$(1 - \beta)[\tan(kl/2) - (kl/2)] = 0. \quad (11)$$

Since the solution $\beta = 1$ yields vanishing bending moment for the entire region, we see that the nontrivial solution for this equation is the transcendental equation

$$\tan(kl/2) = kl/2. \quad (12)$$

The smallest value of kl to satisfy this equation is

$$kl = 8.9870 \quad (13)$$

or

$$Nl^2/EI = (8.9870)^2. \quad (14)$$

If the point of separation is represented by the half angle ϕ^* we have

$$\phi^* = l/2R \quad (15)$$

and equation (14) may be expressed as

$$NR^2\phi^{*2}/EI = (4.4935)^2 = 20.15. \quad (16)$$

This means that, when the region of separation ϕ^* is given the compressive load N can be uniquely determined. By introducing a nondimensional parameter

$$\lambda = pR^3/EI \quad (17)$$

we have

$$\lambda = 20.15 \cdot \beta/\phi^{*2}. \quad (18)$$

The vertical displacement Δ at the plane of symmetry can be calculated from equation (10). In nondimensional form we can write simply

$$\delta = \Delta/R = 0.7775(1 - \beta)\phi^{*2}. \quad (19)$$

To determine the corresponding distributed inertia load, p , it is necessary to calculate the parameter β which represents the ratio of p and N . To determine β we need to introduce the compatibility condition. We assume that there is no friction between the ring and the wall and calculate the circumferential displacement u at the point of separation resulting from the shortening of the attached segment of the ring. We see that the circumferential component of the distributed inertia load is given by $p \sin \phi$. Thus the distribution of the internal compressive force along the ring is

$$F(\phi) = R \int_{\phi^*}^{\phi} p \sin \phi \, d\phi + N = Rp(\cos \phi^* - \cos \phi) + N. \quad (20)$$

The corresponding mid-plane strain is

$$\varepsilon(\phi) = -F(\phi)/EA \quad (21)$$

where A is the cross-sectional area of the ring. The tangential displacement of the point of separation, which is the total shortening for one half of the attached segment (i.e. for $\phi^* < \phi < \pi$) is

$$u(l/2) = - \int_{\phi^*}^{\pi} \varepsilon R \, d\phi = (R/EA)[Rp \cos \phi^* + N](\pi - \phi^*) + Rp \sin \phi^*. \quad (22)$$

Under the present assumption of small ϕ^* we can set $\cos \phi^* = 1$ and $\sin \phi^* = \phi^*$, and obtain

$$u(l/2) = (NR/EA)[(1 + \beta)\pi - \phi^*]. \quad (23)$$

We calculate next the tangential displacement $u(l/2)$ by considering the mid-plane strain of the detached region. For the deformed ring the mid-plane strain can be expressed as

$$\varepsilon(s) = \frac{du}{ds} - \frac{w}{R} + \frac{1}{2} \left(\frac{dw}{ds} \right)^2. \quad (24)$$

Since the internal compressive force N is constant, the mid-plane strain is also constant, i.e.

$$\varepsilon(s) = -N/EA. \quad (25)$$

Since for symmetric deformation the displacement u is zero at the plane of symmetry, we have

$$u(l/2) = \int_0^{l/2} \left[-N/EA + w/R - \frac{1}{2} (dw/ds)^2 \right] ds \quad (26)$$

and by substituting w from equation (10),

$$u(l/2) = -(NR\phi^*/EA) - R\phi^{*3} \left[\frac{5}{12}(1-\beta)^2 - \frac{1}{3}(1-\beta) \right]. \quad (27)$$

From equations (23) and (27) we obtain the following simple compatibility relation:

$$5\beta^2 - 6\beta + 1 + C\gamma(1+\beta)/\phi^{*5} = 0 \quad (28)$$

where

$$\gamma = I/AR^2 \quad (29)$$

and

$$C = 3\pi(kl)^2 = 761. \quad (30)$$

The solution of the present problem, hence, involves simply a quadratic equation. For a ring with a given geometrical parameter γ , in general, two solutions for β can be determined from equation (28) for each value of ϕ^* . Knowing ϕ^* and β , the corresponding distributed load λ and mid-point displacement δ can be calculated respectively by equations (18) and (19).

We note further from equation (28) that the value of β is a function of γ/ϕ^{*5} , while from equations (18) and (19) the values of λ and δ are proportional to $1/\phi^{*2}$ and ϕ^{*2} respectively. This means that for a given value of β , ϕ^* is proportional to $\gamma^{1/5}$, and if the loading and deflection parameters are taken as $\lambda\gamma^{3/5}$ and $\delta\gamma^{-3/5}$ respectively, only one single load-deflection curve will be required to include all cases involving different values of γ . Such a curve is shown in Fig. 2. It can be seen from this figure that a maximum allowable distributed loading of $\lambda\gamma^{3/5}$ equal to 0.73 is reached when $\delta\gamma^{-3/5}$ is equal to 3.7. This corresponds to the snap-buckling load.

It can also be seen that the relation between the point of separation and the mid-point deflection can also be represented by a single curve when $\phi^*\gamma^{-1/5}$ and $\delta\gamma^{-3/5}$ are used as the nondimensional parameters. Figure 3, which presents such a relationship, indicates that the location of the point of separation ϕ^* is moving toward the center when the distributed loading increases gradually; it reaches a limiting value of $\phi^*\gamma^{-1/5}$ equal to 0.43 and begins to move back down the wall.

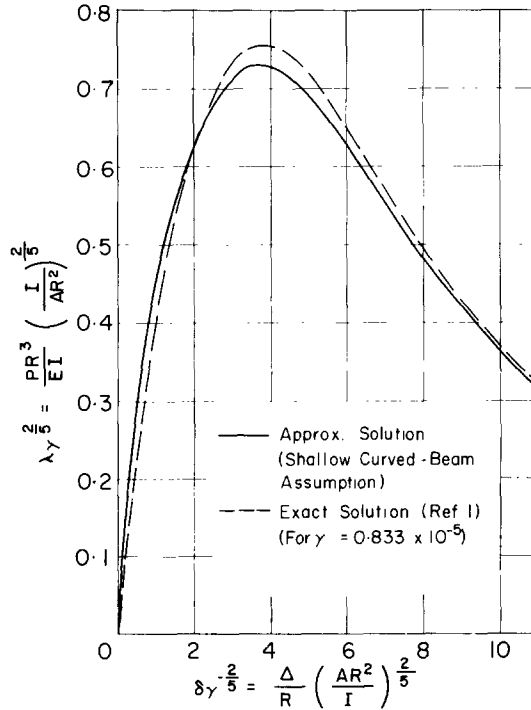


FIG. 2. Loading magnitude vs. mid-point deflection.

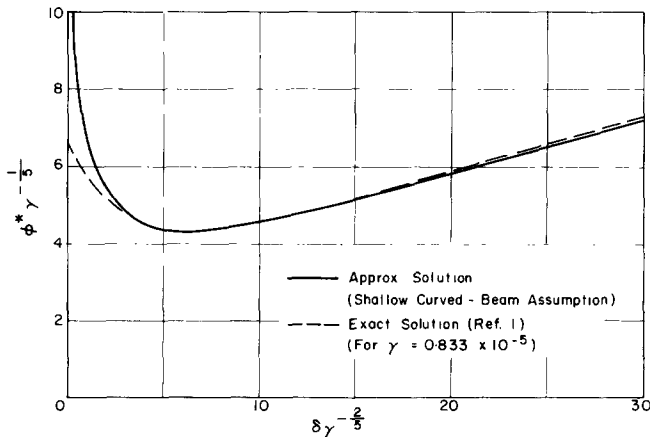


FIG. 3. Point of separation vs. mid-point deflection.

Inextensional rings

It is obvious that Figs. 2 and 3 are not applicable to the limiting case of inextensional rings for which the geometrical parameter γ is zero. For such case equation (28) becomes simply

$$(1 - \beta)(1 - 5\beta) = 0 \tag{31}$$

or

$$\beta = \begin{cases} 1.0 \\ 0.2 \end{cases}.$$

Since the case of $\beta = 1.0$ corresponds to zero displacement, the only solution applicable to the inextensional problem is β equal to 0.2. For this value of β , the following relation between λ and δ can be determined by eliminating the parameter ϕ^* :

$$\delta = 2.5/\lambda \quad (32)$$

Behavior of the approximate solution in the small-deflection range

We can see from Fig. 3 that for small δ the angle of separation ϕ^* becomes large. For small values of $C\gamma/\phi^{*5}$ we can show that the roots of equation (28) approach

$$\beta = \begin{cases} 1 - \frac{1}{5} \frac{C\gamma}{\phi^{*5}} \\ \frac{2}{10} + \frac{3}{10} \frac{C\gamma}{\phi^{*5}} \end{cases} \quad (33)$$

Of these two roots, the first one is associated with the small deflection problem. Thus from equations (18) and (19) we can show that ϕ^* approaches infinity when δ approaches zero and the mid-point deflection δ is proportional to $\lambda^{\frac{3}{2}}$ in the small deflection range. This means that the initial slope for the λ vs. δ curve is infinite as shown in Fig. 3.

We should, however, recognize that for large values of ϕ^* the present approximate formulation is no longer valid. Thus we need an exact formulation to determine the behavior of the ring in the small deflection range. This exact small deflection linear analysis is presented in the next section.

SMALL DEFLECTION LINEAR ANALYSIS

When the radial displacement w is small in comparison to the ring thickness, formulation of the equilibrium equation based on the undeformed condition is justifiable. Let H and V be the horizontal and vertical reactions at the point of separation as shown in Fig. 4. With the condition of vanishing bending moment at the boundary we can write the bending moment distribution in the following form

$$M(\phi) = -VR(\sin \phi^* - \sin \phi) + HR(\cos \phi - \cos \phi^*) + \int_{\phi}^{\phi^*} p(\sin \theta - \sin \phi)R^2 d\theta \quad (34)$$

where ϕ and θ are angles measured from the vertical axis and ϕ^* is the angle at the point of separation. By substituting $V = Rp\phi^*$, we obtain

$$M(\phi) = pR^2(\phi \sin \phi - \phi^* \sin \phi^*) + (pR^2 + HR)(\cos \phi - \cos \phi^*). \quad (35)$$

The distribution of the internal compressive force is given by

$$N(\phi) = H \cos \phi + pR\phi \sin \phi. \quad (36)$$

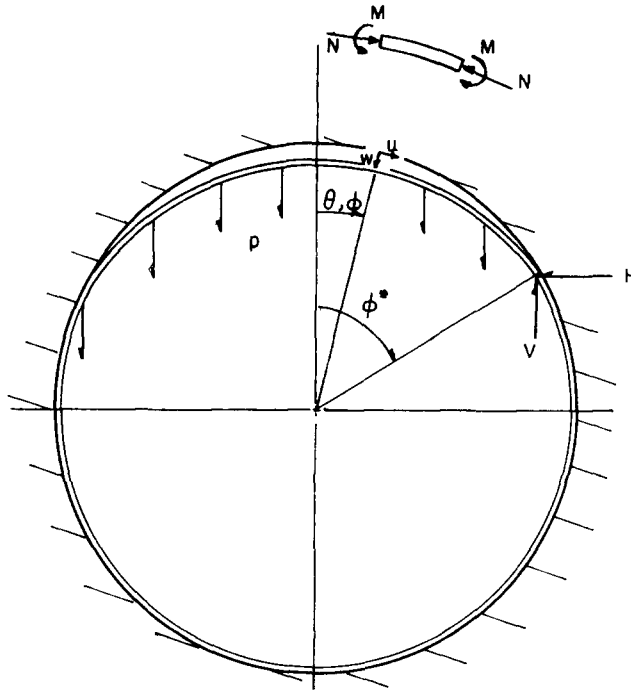


FIG. 4. Small deflection ring configuration.

We introduce next the moment-curvature relationship and the relation between the internal compressive force and the mid-plane strain:

$$M(\phi) = \frac{EI}{R^2} \left(\frac{d^2 w}{d\phi^2} + \frac{du}{d\phi} \right) \quad (37)$$

and

$$N(\phi) = \frac{EA}{R} \left(w - \frac{du}{d\phi} \right). \quad (38)$$

By combining equation (35) with equation (37) and equation (36) with equation (38) and by introducing the following new nondimensional parameters

$$U = u/R \quad W = w/R \quad (39)$$

and

$$\omega = H/pR \quad (40)$$

we obtain

$$\frac{d^2 W}{d\phi^2} + \frac{dU}{d\phi} = \lambda [(\phi \sin \phi - \phi^* \sin \phi^*) + (1 + \omega)(\cos \phi - \cos \phi^*)] \quad (41)$$

and

$$W - \frac{dU}{d\phi} = \lambda\gamma(\phi \sin \phi + \omega \cos \phi). \quad (42)$$

The boundary conditions are:

- (1) at $\phi = 0$ $U = 0$
- (2) at $\phi = 0$ $dW/d\phi = 0$
- (3) at $\phi = \phi^*$ $W = 0$ (43)
- (4) at $\phi = \phi^*$ $dW/d\phi = 0$
- (5) at $\phi = \phi^*$ $U = \lambda\gamma\{(\pi - \phi^*)[(1 + \omega) \cos \phi^* + \phi^* \sin \phi^*] + \sin \phi^*\}$.

The right-hand side of the last condition is the shortening of the attached segment from $\phi = \phi^*$ to $\phi = \pi$. It is determined from equation (22) by replacing N by

$$H \cos \phi^* + pR\phi^* \sin \phi^*.$$

We can see that U can be eliminated from equations (41) and (42) to form a single differential equation for W . We notice here, however, that for thin rings the parameter γ is much less than unity; hence the term involving γ may be neglected. The differential equation for W is, thus, simply

$$\frac{d^2 W}{d\phi^2} + W = \lambda[(\phi \sin \phi - \phi^* \sin \phi^*) + (1 + \omega)(\cos \phi - \cos \phi^*)]. \quad (44)$$

This is a second-order differential equation containing two unknown quantities ω and ϕ^* . The three boundary conditions for W , in fact, permit the evaluation of the two integration constants and the third constant ω .

The solution of equation (44) is

$$W = \lambda \left\{ A \sin \phi + B \cos \phi - [\phi^* \sin \phi^* + (1 + \omega) \cos \phi^*] + \left(\frac{1}{4} + \frac{1 + \omega}{2} \right) \phi \sin \phi - \frac{1}{4} \phi^2 \cos \phi \right\} \quad (45)$$

and the three constants are

$$A = 0 \quad (46)$$

$$B = \frac{\phi^{*3} + \frac{1}{2}\phi^{*2} \sin 2\phi^* + \phi^*(3 - \cos 2\phi^*) - \sin 2\phi^*}{4\phi^* - 2 \sin 2\phi^*} \quad (47)$$

and

$$\omega = \frac{\sin 2\phi^* - 2\phi^* \cos 2\phi^*}{4\phi^* - 2 \sin 2\phi^*}. \quad (48)$$

To determine the angle of separation ϕ^* we need to integrate equation (42). Here, of course, the term involving γ can not be neglected. We have

$$U(\phi^*) = \int_0^{\phi^*} \frac{dU}{d\phi} d\phi \\ = \int_0^{\phi^*} W d\phi - \lambda\gamma \int_0^{\phi^*} (\phi \sin \phi + \omega \cos \phi) d\phi. \quad (49)$$

After substituting $W(\phi)$ from equation (45) and equating $U(\phi^*)$ with that given in the last condition of equations (43), we obtain (after considerable simplifying),

$$\gamma\pi[(1 + \omega) \cos \phi^* + \phi^* \sin \phi^*] = (1 - \gamma)[-(2 + \omega)\phi^* \cos \phi^* + (2 + \omega - \phi^{*2}) \sin \phi^*] \quad (50)$$

The factor γ in the right hand side of the equation, of course, can be neglected here. The final equation to be used to evaluate ϕ^* is the following transcendental equation:

$$\gamma\pi[(1 + \omega) \cos \phi^* + \phi^* \sin \phi^*] = -(2 + \omega)\phi^* \cos \phi^* + (2 + \omega - \phi^{*2}) \sin \phi^* \quad (51)$$

where $\omega(\phi^*)$ is given by equation (48).

We observe that the values of the various constants in this solution such as ω , B and ϕ^* are all independent of the magnitude of the distributed load λ , and that, from equation (45), the radial displacement $W(\phi)$ is linearly related to the loading magnitude. This behavior is clearly different from that predicted by the previous approximate solution.

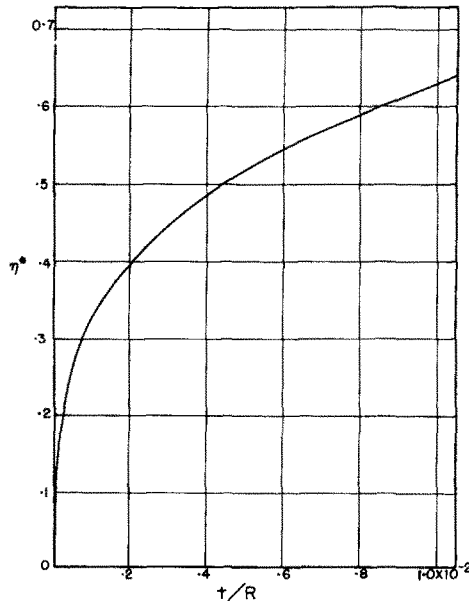


FIG. 5. Effect of ring thickness on initial angle of separation.

Equation (51) has been solved for various values of γ and the results have been plotted in Fig. 5. It is seen that, when γ approaches zero, the angle of separation also approaches zero. This means that if the ring is inextensional there can be no radial displacement under the small deflection theory.

EXACT FORMULATION

Finally, let us discuss the exact formulation in which we consider the possibility of very large ring deflection. By letting \bar{s} be the distance measured from the symmetrical axis along the circumference of the deformed ring as shown in Fig. 6, we obtain the following equation of equilibrium:

$$\frac{dM}{d\bar{s}} = Q \quad (52)$$

where M is the bending moment and Q is the transverse shear. The latter can be resolved into its horizontal and vertical components H and V , i.e.

$$Q = H \sin \psi - V \sin \psi \quad (53)$$

where ψ is the angle that a tangent of the deformed ring makes with the horizontal axis.

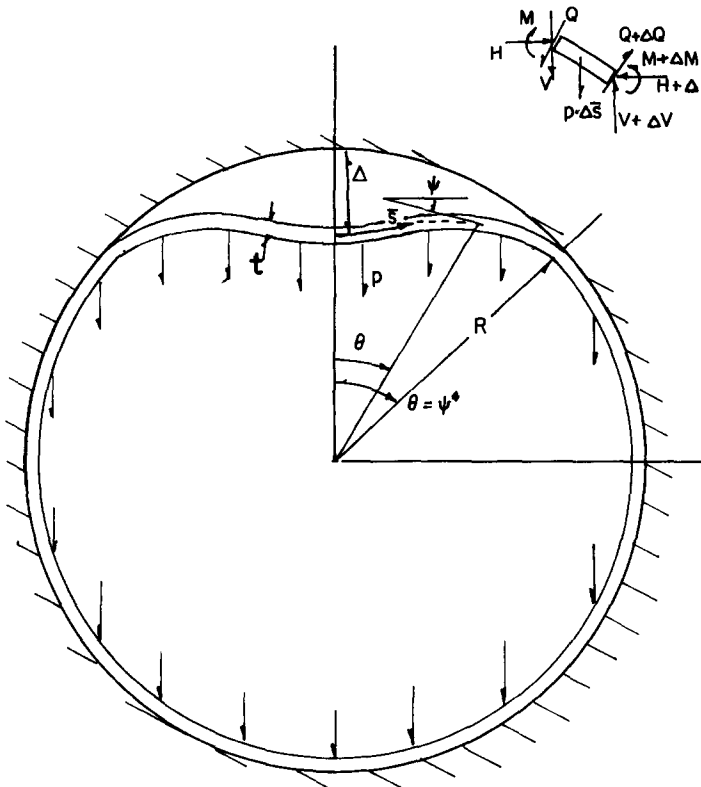


FIG. 6. Large deflection ring configuration.

We see that the horizontal force H is a constant equal to the horizontal reaction at the point of separation while

$$V = p\bar{s} \quad (54)$$

where p = distributed load per unit length.

We introduce next the moment-curvature relation

$$M/EI = \frac{1}{R} - \frac{d\psi}{d\bar{s}} \quad (55)$$

and obtain

$$\frac{d^2\psi}{d\bar{s}^2} = \frac{1}{EI}(p\bar{s} \cos \psi - H \sin \psi) \quad (56)$$

In nondimensional form this equation becomes

$$\frac{d^2\psi}{d\eta^2} = \lambda(\eta \cos \psi - \omega \sin \psi) \quad (57)$$

where

$$\eta = \bar{s}/R \quad (58)$$

and λ and ω are defined in the same manner as before.

Letting the value of η at the point of separation be η^* , we have the following boundary conditions for equation (56):

$$\text{at } \eta = 0, \quad \psi = 0 \quad (59)$$

$$\text{at } \eta = \eta^*, \quad d\psi/d\eta = 1. \quad (60)$$

Since both ω and η^* are unknown we find that we need two additional conditions. These conditions can be obtained from the compatibility requirements. The first requirement follows from the assumption of symmetric deformation, namely the horizontal component of the displacement at $\eta = 0$ must vanish. This condition takes the form

$$R \sin \psi^* = \int_0^{\bar{s}^*} \cos \psi \, d\bar{s} \quad (61)$$

where ψ^* and \bar{s}^* are the corresponding quantities at the point of separation. In nondimensional form this is

$$\sin \psi^* = \int_0^{\eta^*} \cos \psi \, d\eta. \quad (62)$$

The second compatibility condition is concerned with the tangential displacement at the point of separation. The compressive force in the detached segment is given by

$$F(\psi) = H \cos \psi + p\bar{s} \sin \psi. \quad (63)$$

Thus the total shortening for the segment between $\bar{s} = 0$ and $\bar{s} = \bar{s}^*$ is

$$\Delta_1 = \frac{1}{AE} \int_0^{\bar{s}^*} F \, d\bar{s} = \frac{1}{AE} \int_0^{\bar{s}^*} (H \cos \psi + p\bar{s} \sin \psi) \, d\bar{s} \quad (64)$$

and in nondimensional form

$$\Delta_1/R = \lambda \int_0^{\eta^*} (\omega \cos \psi + \eta \sin \psi) \, d\eta. \quad (65)$$

Let θ^* be the angular location of the point of separation in the original undeformed configuration. We have

$$\theta^* = \eta^* + \Delta_1/R. \quad (66)$$

The angle θ^* may also be related to the shortening Δ_2 of the attached segment, i.e.

$$\theta^* = \psi^* - \Delta_2/R \quad (67)$$

where Δ_2/R is the nondimensional displacement $U(\phi^*)$ and has been given by the last equation of equation (43). Under the present notation ϕ^* should be replaced by ψ^* , i.e.

$$\Delta_2/R = \lambda\gamma\{(\pi - \psi^*)[(1 + \omega) \cos \psi^* + \psi^* \sin \psi^*] + \sin \psi^*\}. \quad (68)$$

Combining equations (65), (66), (67) and (68) we obtain the following compatibility condition

$$\begin{aligned} \psi^* - \eta^* = \lambda\gamma \left\{ (\pi - \psi^*)[(1 + \omega) \cos \psi^* + \eta^* \sin \psi^*] \right. \\ \left. + \sin \psi^* + \int_0^{\eta^*} (\omega \cos \psi + \eta \sin \psi) d\eta \right\}. \end{aligned} \quad (69)$$

We see that, under the exact formulation, the solution of the present problem is reduced to the determination of $\psi(\eta)$, η^* and ω for any given λ by means of equations (57), (59), (60), (62) and (68). This set of nonlinear equations is solved by an iterative procedure given in the following section.

To prepare for the iterative procedure we perform first the following operation: Multiplying equation (57) by η , integrating the left-hand side by parts and applying the boundary conditions given by equations (59) and (60), we obtain

$$\frac{\psi^* - \eta^*}{\lambda} = - \int_0^{\eta^*} \eta[\eta \cos \psi - \omega \sin \psi] d\eta \quad (70)$$

Eliminating $(\psi^* - \eta^*)/\lambda$ from equations (69) and (70) and solving for ω , we obtain an expression of the following form:

$$\omega = \frac{C_2 + \gamma(S_1 + a)}{S_1 - \gamma(C_0 + b)} \quad (71)$$

where

$$a = (\pi - \psi^*)(\cos \psi^* + \eta^* \sin \psi^*) + \sin \psi^* \quad (72)$$

$$b = (\pi - \psi^*) \cos \psi^* \quad (73)$$

and S_n and C_n are integrals defined by

$$C_n \equiv \int_0^{\eta^*} \eta^n \cos \psi d\eta \quad (74)$$

$$S_n \equiv \int_0^{\eta^*} \eta^n \sin \psi d\eta. \quad (75)$$

It is seen that with the symbols so defined, the compatibility condition given by equation (69) may be written as

$$\psi^* = \eta^* + \lambda v[\omega(b + C_0) + a + S_1] \quad (76)$$

Iterative solution

The iterative procedure used to solve the system of nonlinear equations is similar to what has been termed Newton's method [2]. The technique, as it is applied here, involves two steps: (i) establish a nominal solution which satisfies the nonlinear differential equation and part of the boundary and auxiliary conditions; (ii) a correction for this solution is obtained by solving the linear nonhomogeneous "variational equations" for the nonlinear system of equations. This correction is used to compute a new nominal solution and the process is repeated until the correction approaches zero.

The present system of nonlinear equations involves not only an unknown coefficient ω but also an unidentified boundary location η^* . In the present solution of the problem, however, η^* is assumed given while the function $\psi(\eta)$ and the two constants ω and λ are to be evaluated. The following procedure is adopted in the establishment of the nominal solution, $\bar{\psi}(\eta)$, $\bar{\lambda}$, and $\bar{\omega}$.

We assume a function $\psi(\eta)$ that we expect might constitute a possible equilibrium configuration. The solutions of the approximate formulation which were discussed earlier are, of course, the logical trial-solutions. We may also make use of the already converged solution for one value of η^* and apply a simple scaling factor to obtain the trial solution for a neighboring value of η^* .

Having chosen η^* and a trial solution, $\psi(\eta)$, we can evaluate the constants a and b and, by numerical integration, the quantities C_0 , C_2 and S_1 . From equation (71) we can evaluate $\bar{\omega}$, and by assuming a value for ψ^* , we can determine $\bar{\lambda}$ by means of equation (76). Using this value of ψ^* and equation (60) as initial conditions, we can then numerically integrate equation (57) using a Runge-Kutta scheme. From the new function $\psi(\eta)$ and the determined values of $\bar{\lambda}$ and $\bar{\omega}$, a new value of ψ^* can be found from equation (76). Equation (57) can be integrated again and the process repeated until ψ^* settles down to some asymptotic value. The final function $\bar{\psi}(\eta)$ together with $\bar{\lambda}$ and $\bar{\omega}$, constitutes the nominal solution. It is seen that this solution satisfies equations (57), (60) and (69) but it does not satisfy the conditions given by equations (59) and (62). Thus there are two measures of error associated with this solution.

$$e_1 = \int_0^{\eta^*} \cos \psi \, d\eta - \sin \psi^* \quad (77)$$

$$e_2 = \psi(0) \quad (78)$$

To reduce these errors we consider small perturbations of $\bar{\psi}(\eta)$, $\bar{\lambda}$ and $\bar{\omega}$, the nominal solution, and write

$$\psi(\eta) = \bar{\psi}(\eta) + \xi(\eta) \quad (79)$$

$$\lambda = \bar{\lambda} + \delta\lambda \quad (80)$$

$$\omega = \bar{\omega} + \delta\omega \quad (81)$$

Substituting the above into equations (57) and (69) and neglecting the quadratic terms in ξ , $\delta\lambda$ and $\delta\omega$ we obtain the following linear equations for $\xi(\eta)$, $\delta\lambda$ and $\delta\omega$

$$\frac{d^2\xi}{d\eta^2} + \bar{\lambda}[\eta \sin \bar{\psi} + \bar{\omega} \cos \bar{\psi}] \xi(\eta) = \delta\lambda(\eta \cos \bar{\psi} - \bar{\omega} \sin \bar{\psi}) - \delta\omega(\bar{\lambda} \sin \bar{\psi}) \tag{82}$$

$$0 = \xi^* \left[\eta^*(\bar{b} - \sin \bar{\psi}^*) + (1 + \bar{\omega})(\pi - \bar{\psi}^*) \sin \bar{\psi}^* - \bar{\omega} \cos \bar{\psi}^* - \frac{1}{\bar{\lambda}_\gamma} \right] + \frac{\delta\lambda}{\bar{\lambda}} [\bar{a} + \bar{S}_1 + \bar{\omega}(\bar{b} + \bar{C}_0)] \tag{83}$$

where \bar{a} , \bar{b} , \bar{C}_0 and \bar{S}_1 are also associated with the nominal solution.

In order for $\psi(\eta)$ to satisfy equations (78), (60) and (77), we must have

$$\xi = -e_2 \quad \text{at } \eta = 0 \tag{84}$$

$$\frac{d\xi}{d\eta} = 0 \quad \text{at } \eta = \eta^* \tag{85}$$

and

$$\int_0^{\eta^*} \xi \sin \bar{\psi} \, d\eta - \xi^* \cos \bar{\psi}^* = e_1. \tag{86}$$

We now assume $\xi(\eta)$ in the form

$$\xi(\eta) = -e_2 + \sum_{i=1}^n b_i \eta^i \tag{87}$$

where the constant term has been chosen such that equation (84) is satisfied. The value of ξ at the point of separation is

$$\xi^* = -e_2 + \sum_{i=1}^n b_i (\eta^*)^i \tag{88}$$

We now insure that equation (82) is satisfied in the mean by taking moments of this equation. The number of moment equations required depends upon the number of unknown coefficients appearing in equation (87). We may now treat $\delta\omega$, $\delta\lambda$, ξ^* , b_1, \dots, b_n as unknowns and hence in addition to equations (85), (88), (86) and (83) we need $(n - 1)$ moment equations. In this effort n was taken as 4 so that we have a system of 7 linear equations in the 7 unknowns $\delta\omega$, $\delta\lambda$, ξ^* , b_1, \dots, b_4 .

Upon solution of this system of equations, we can compute new values for $\psi(\eta)$, $\bar{\lambda}$ and $\bar{\omega}$ from equations (79), (80) and (81). This solution, however, will in general not satisfy the compatibility relationship, equation (76). To insure that this condition is satisfied, we again cycle through the numerical integration of equation (57) and the evaluation of ψ^* from equation (76) until ψ^* approaches some asymptotic value. We have, at this point, a new nominal solution and two new measures of error, e_1 and e_2 . The iterative procedure is repeated until both of these measures have been reduced to negligible small numbers.

COMPARISON OF RESULTS OF EXACT AND APPROXIMATE FORMULATIONS

Using the iterative procedure, an exact load-deflection curve has been determined for a single value of the geometrical parameter γ , equal to 0.833×10^{-5} . This solution has been plotted in terms of $\lambda\gamma^{\frac{2}{3}}$ vs. $\delta\gamma^{-\frac{2}{3}}$ in Fig. 2. The corresponding plot for the location of the point of separation has also been presented as $\phi^*\gamma^{-\frac{2}{3}}$ vs. $\delta\gamma^{-\frac{2}{3}}$ in Fig. 3. It should be pointed out that the solution for the small deflection range agrees very well with the results of the small-deflection linear analysis.

It is seen that, for this value of γ , the comparison between the approximate and exact solution is quite satisfactory. The approximate method predicts a snap-buckling load which is lower by about three percent in comparison to the exact result. For this value of γ , the value of ϕ^* at the snap-buckling load is approximately 0.45 radians. Hence it is within expectation that the shallow curved-beam assumption would be satisfactory for rings of this geometry. Figure 3, however, indicates that for rings of smaller R/t , the point of separation ϕ^* may attain larger values. Thus, one would expect less accurate results for thicker rings using the approximate solution.

REFERENCES

- [1] L. L. BUCCIARELLI, JR. and T. H. H. PIAN, Symmetric deformation of a radially-constrained thin circular ring under inertia loading. Massachusetts Institute of Technology, Aeroelastic and Structures Research Laboratory, ASRL TR 127-1 (AFOSR 65-1619) July 1965.
- [2] G. A. THURSTON, *J. appl. Mech.* **30**, 383 (1963).

(Received 18 July 1966; revised 10 February 1967)

Résumé—L'exposé présente d'abord une solution approximative de la déformation statique, élastique d'un anneau circulaire mince qui est soumis à la contrainte d'une limite circulaire rigide et est soumis à l'action d'une charge distribuée uniformément de long d'une direction dans le plan de l'anneau. La solution est basée sur la supposition que la région détachée se limite à une petite partie de la circonférence. Le résultat de la solution est représenté par une courbe de déviation de la charge qui indique le comportement de l'anneau quant à la rupture et au fléchissement.

Le système d'équation non linéaire pour la formulation exacte a aussi été étudié. Un plan systématique itératif est développé pour sa solution et est appliqué à un anneau de R/t égal à 100. Le résultat peut être comparé favorablement à la solution approximative.

Zusammenfassung—Diese Arbeit gibt zunächst Annäherungslösungen der statisch-elastischen Formveränderung eines dünnen Kreisringes, der in einer starren ringförmigen Aushöhlung gehalten wird, und auf den gleichmässig verteilte Belastungen in der Richtung der Ringebene einwirken. Die Lösung beruht auf der Voraussetzung, dass der unabhängige Bereich auf einen kleinen Teil des Umfanges beschränkt ist. Die Lösungen werden dargestellt als eine lastabhängige Kurve die das Durchschlag-Knick Verhalten des Ringes anzeigt.

Das nichtlineare Gleichungssystem zur genauen Bestimmung wurde auch untersucht. Ein systematisches sich wiederholendes System der Lösung wurde entwickelt und wird angewandt auf einen Ring mit $R/t = 100$. Das Resultat ist gut im Vergleich mit der Annäherungslösung.

Абстракт—В работе представлено, в первые, приближенное решение статической, упругой деформации тонкого, круглого кольца, которое является несвободным на жесткой, круглой границе и находится под действием равномерно распределенной нагрузки, направленной в плоскости кольца. Решение основано на предположении, что обособленный район ограничен малой частью окружности. Результат решения представлен кривой: нагрузкапрогиб, которая указывает на внезапное выпучивание кольца.

Исследуется также система нелинейных уравнений при строгой формулировке. Выведено систематическую схему последовательных приближений для решения этих уравнений и применено к кольцу, в котором отношение R/t равняется 100. Результат показывает надлежащее согласие с приближенным решением.